AUTOMATED QUANTITATIVE ANALYSIS OF CONFOCAL IMAGES OF NEURONAL NETWORK CULTURES

H. Dinh[1]*, D. Jimenez*[1]*, E. Papadakis*[1]*, F. Laezza*[2]*, D. Labate*[1]

[1]Department of Mathematics, University of Houston,
[2]Department of Pharmacology and Toxicology, The University of Texas Medical Branch

ABSTRACT

High resolution confocal imaging enables the study of structure-function correlations linking molecular features of neurons to their functional output. However, current analysis and processing tools still require a very significant manual intervention, making it impractical or impossible to conduct the large-scale analysis which is often needed for integrated predictive models of single-cell and large neuronal networks function. In this paper, we present a pilot study towards the development of a fully scalable large-scale processing framework enabling the automated computation of structure-function associative measurements of neuronal proteins in subcellular compartments from 3D confocal imagery.

1. INTRODUCTION

High resolution confocal imaging has become an indispensable tool in molecular neuroscience enabling to capture morphological features of neurons and to track the sub-cellular distribution and dynamics of neuronal proteins at nanoscale level in both cultured preparations and in vivo. Yet, while these state-of-art methodologies have opened new avenues towards the understanding of structure-function correlations linking molecular features of neurons to their functional output, the lack of rapid and accurate methods for image analysis has hampered the use of confocal imaging for large-scale studies. Current image analysis and processing software, indeed, still require a significant manual intervention, which is a critical limiting factor for the extraction of accurate measurements from complex and voluminous data that are essential for establishing reliable predictive models of the basic mechanisms of neuronal function.

Neurons adapt their functional output in response to stimuli through a dynamic remodeling of their protein content and sub-cellular distribution, a process that is severely altered in brain disorders [7]. A critical player in these adaptive mechanisms is the macromolecular complex of the voltage-gated Na+ (Nav) channel complex and its associated proteins at the axonal initial segment (AIS), the site of initiation of the action potential. Emerging evidence indicates that this protein-protein interaction complex can undergo a structural remodeling that underlies plastic adaptations of neuronal excitability, and, if aberrant, leads to neurodegenerative processes and cell death. To facilitate the understanding of this molecular mechanism, it is critical to accurately estimate the spatial distribution of the Nav channel protein complex at AIS from high-resolution imaging.

In this paper, we introduce a multistep strategy aiming at providing an automated computational platform for large-scale analysis of the spatial distribution of specific ion channel complexes in sub-cellular compartments from confocal images. Our approach will combine state-of-the-art image processing tools, including data denoising, segmentation and centerline tracing, together with a novel routine specifically designed for the extraction of associative measures relative to fluorescently-labeled proteins of interest (analytes). We envision that, once fully completed, this platform will enable a multimodal integration of data from confocal imaging, electrophysiological measurements and other functional assays in simulation environments (such as NEURON [2] or GENESIS [1]) towards an integrated predictive model of single-cell and large neuronal networks function.

2. BIOLOGICAL PREPARATION

Primary neuronal cultures. Primary hippocampal neurons were prepared from embryonic rat brains (E18) and maintained on coverslips in close proximity of an astrocyte glia feeder layer for 2-3 weeks, as previously described [6].

Immunofluorescence staining. Neurons were fixed in 4% paraformaldehyde/4% sucrose and incubated with the following combination of primary antibodies: rabbit anti-microtubule-associated protein 2 (MAP2; 1:500, Chemicon), rabbit anti-PanNav subunit (1:100, Sigma), mouse anti-FGF14 protein (1:200, NeuroMab). After washing, neurons were stained with appropriate Alexa 563 and 647-conjugated secondary antibodies (Invitrogen), mounted on glass coverslips and processed for confocal image acquisition.

Image acquisition. Confocal images were acquired with a Zeiss 510 laser scanning microscope (Zeiss, Oberkochen, Germany) using a 63x oil immersion objective (1.4 numerical aperture). For manual analysis, stacked images were analyzed with the open source ImageJ software using a line scan method, by highlighting a line of 6 pixels in width and 20 μm

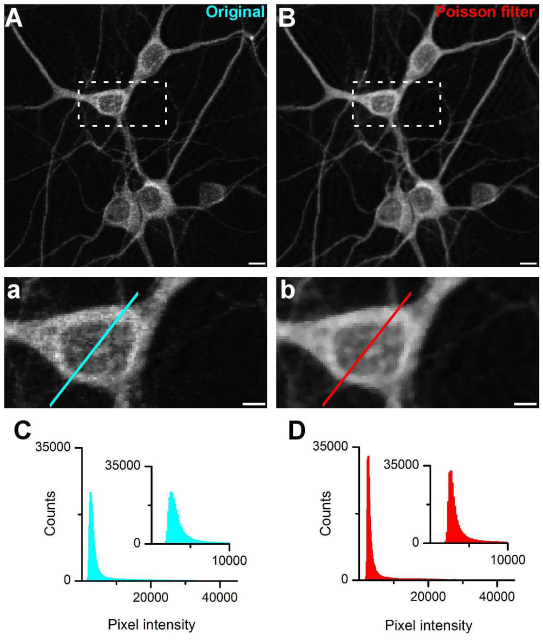

Fig. 1. Confocal images are preprocessed to remove degradation using a thresholding scheme based on shearlets. C,D: The denoising filter does not affect the overall pixel intensity distribution in the image. The small inset a,b provides a better visualization of pixel distribution. Scale bar= $5\mu m$

in length along MAP2-negative process (AIS) and MAP2-positive process (dendrites) on the Alexa 568 images corresponding to Nav channels.

3. A MULTISTEP PROCESSING PLATFORM

We present a computational platform for the automated computation of the spatial distribution of macromolecular complexes of interest in specific subcellular regions of confocal images of neurons. This platform is organized into the following sequence of processing stages.

1. *Data preprocessing*. Images acquired through confocal microscopy are affected by several sources of degradation and need to be restored in order to facilitate the segmentation stage which is needed for extracting the centerlines of processes of interest and computing the associative measures. Such degradation includes the blurring due to the convolution of the original signal intensities with the point spread function of the imaging system and the noise introduced by the stochastic nature of the photon-counting process at the detector, which can be modeled as a Poisson-distributed random process. To address that, we use a denoising algorithm based on shearlets and adaptive thresholding, previously developed by one of the author and his collaborators [3, 8]. This approach is especially suitable to this type of data, since shearlets are especially designed to represent anisotropic objects efficiently [3] (`www.math.uh.edu/~dlabate/software.html`). A demonstration of the denoising algorithm is shown in Figure 1 showing that the algorithm does not degrade the curvilinear features of the data. Denoised data are used in the successive stage of segmentation and centerline extraction.

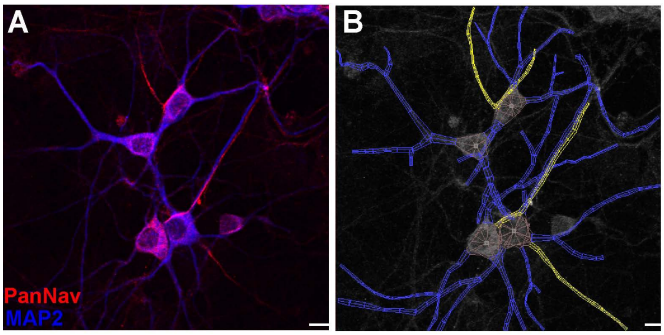

Fig. 2. Neurons are segmented and traced using Neuromantic. Image A shows the overlay confocal image of cultured hippocampal neurons immunolabeled for the Nav channel α subunits (red) and the microtubule-associated protein, MAP2 (blue), used as a marker of the somato-dendritic compartment. Note that the red fluorescence signal is concentrated in thin neuronal processes representing the AIS, while is dimmer in the somato-dendritic compartment visualized through the blue channel. Segmented data and centerline are shown in B, where structures from blue and red channels are segmented and traced separately. Scale bar= $5\mu m$

2. *Segmentation and centerline extraction.* Centerline tracing of neurites from confocal images is an essential tool for the construction of the geometrical representation of neurons. It consists, essentially, in generating a graph of points (i.e., the *tracing*) through the midlines of the dendrites and axons of 3D confocal images of neurons. In our framework, centerline tracing provides the necessary spatial reference system for the computation of the associative measures of neurons which are the objective of the next processing stage.

Despite the significant advances in recent years (consider, for example, the methods proposed to address the DIADEM challenge [9]), automated centerline tracing in neurons is still a major bottleneck [4] and we found that none of the available software was completely satisfactory for the type of date we considered. The main limitations we found are not only significant inaccuracies in the form of false positive and negative reconstructions, but also that the current software does not allow to automatically and reliably identify specific subcellular regions such as the AIS, in the way it was needed for the successive computation of associative measures. As a result, in order to focus on the automated computation of associative measures, in this paper we have used Neuromantic (reading.ac.uk/neuromantic/) to manually segment a number

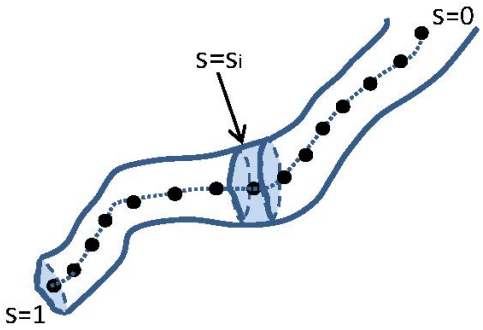

Fig. 3. A typical trace (the dotted line in the figure) is parametrized as a functions of the arc length variable s, $0 \leq s \leq 1$ and the local average intensity is evaluated by computing the average intensity value over cylindrical regions centered at coordinate points $C(s_i)$ sampled along the trace curve.

of representative confocal images of neurons and extract and label their centerline traces (one typical example is given in Figure 2). In Section 4, we discuss in more detail the challenges in developing a fully automated centerline tracing algorithm integrated into the framework presented in this paper and how we plan to address it in the future.

3. *Computation of associative measures.* The goal of this processing stage is to automatically compute functions of the fluorescent intensity associated with specific subcellular compartments of neurons. In the following, we illustrate the computation of the local average fluorescent intensity, measured along the AIS or the proximal section of a dendrites. This algorithm can be easily adapted to other functions.

The algorithm is illustrated with the help of Figure 3. The trace curve C of a neurite is parametrized as a function of the arc length $s \in [0, 1]$. That is, $C(0)$ is the spatial coordinate of the initial point of the neurite and $C(1)$ the spatial coordinate of the terminal point of the neurite (or, of the portion of interest of the neurite). First, C is partitioned into L (disjoint) sections of equal length, that is, $C = \cup_{i=1}^{L} C_i$, where each section C_i is centered at the coordinate $C(s_i)$. Then, the average intensity value is computed on a cylindrical region aligned with C_i, of radius r_i. The value r_i (which is allowed to change in each section) is estimated from the segmentation process of the previous stage.

The algorithm was implemented in Matlab and a typical example of its application is illustrated in Figures 4 and 5. Figure 4 illustrates the selection of one AIS (in yellow) and one dendrite (in blue) from a confocal image which was previously segmented and traced. The algorithm computing the local average fluorescent intensity along the trace of the AIS and the dendrite was run on the red channel of confocal imaging data, as a way to estimate the distribution of Nav channels. The output of the algorithm is plotted in Figure 5 and was

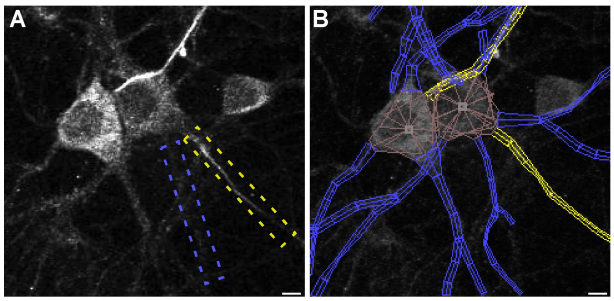

Fig. 4. Preparation for the automated computation of average fluorescent intensity values at the AIS and along a dendrite. In A,B: an axon (yellow) and a dendrite (blue) are selected from a previously segmented images. Scale bar=5 mm

validated against the corresponding intensity profiles computed manually by experts. To remove the effect of the background on the fluorescent intensity measures, the computed values have been corrected by subtracting the intensity level estimated in the regions immediately adjacent the segmented neurite. Corrected measures are reported in color in Figure 5, while uncorrected measures are in black.

The results reported in Figure 5 are similar to several other numerical tests which are not reported here for reasons of space and which demonstrate that our approach for the automated computation of the local average fluorescent intensity at specific neurites is efficient and reliable. Not only does this approach reduce the manual effort in computing these measures, but it also ensure more accurate estimates through the local removal of the background intensity.

4. FURTHER EXTENSIONS AND CONCLUSION

The development of a fully automated framework for the computation of associative measures from confocal images of neurons is still limited by the lack of an automated image processing routine which can reliably an accurately (i) segment the neurons; (ii) label each neuron; (iii) for each neuron, identify the compartments of interest, namely, the soma, the AIS and the dendrites. As mentioned above, several methods have been proposed for segmentation of neuronal structures and centerline tracing, yet they still have serious limitations when dealing with confocal images of neurons, due to the significant presence of noise, the non-uniformity of the intensity levels in the image and the complexity of the morphological structures to recover. Furthermore, the automated labeling of specific neuronal compartments, namely, soma, axons and dendrites is not very reliable. In an effort to address these challenges, we have recently introduced a novel algorithm for segmentation and centerline extraction that is highly accurate and very competitive against current state-of-the art methods [5]. This approach uses of a collection of specially designed multiscale filters for a fast and efficient binarization of neu-

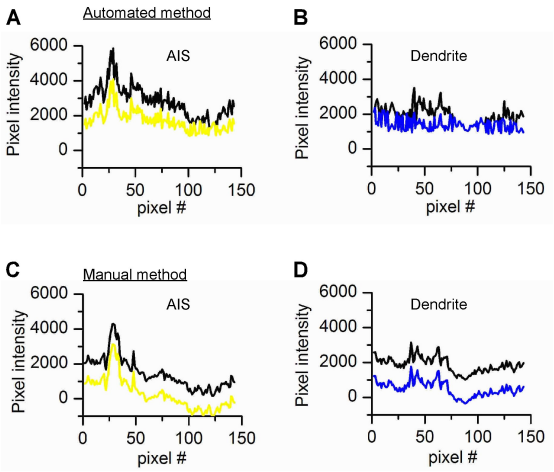

Fig. 5. Local averages of the fluorescent intensity values are automatically computed using our algorithm. Plots A-B show the automatically computed average intensity values at the AIS and at the dendrite of Figure 4 plotted as function of the pixel locations of the centerline trace. The black curve represents the computed intensity without any correction. The color curves show the intensity values after background is subtracted. Plots C-D show the average intensity values at the AIS and at the dendrite manually computed by experts. In this case, the background is estimated as a uniform value for the whole image.

rites in both 2D and 3D. Figure 6 shows the application of this routine to the segmentation of the data of Figure 2A. The integration of this algorithm within the multistep framework for the automated computation of associative measures of analytes in neurons will be the objective of a future endeavour.

In this work, we set the stage for developing a multistep automated procedure for the computation of intensity profiles in targeted subcellular compartments of neurons. This method includes a denoising routine to preprocess confocal images, a segmentation and tracing step and a specifically designed computational routine which computes fluorescent intensity values in specific regions of interests. This work is a pilot study for the development of a fully scalable automated large-scale processing framework enabling the computation of structure-function associative measurements at the AIS from 3D confocal imagery. By enabling the computation of structure-function associative measurements on a large batch of data, this framework will facilitate the understanding of the molecular mechanisms transducing external stimuli into functional neuronal outputs.

5. REFERENCES

[1] J. M. Bower, and D. Beeman. The Book of GENESIS: Exploring Realistic Neural Models with the GEneral NEural SImulation System, Springer, 1998.

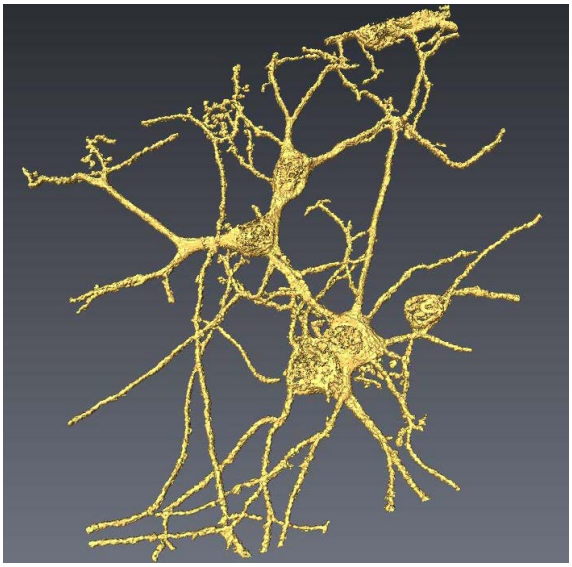

Fig. 6. Example of our automated 3D segmentation.

[2] N. T. Carnevale, and M. L. Hines. *The NEURON book.* Cambridge Univ. Press, 2006.

[3] G. Easley, D. Labate and W. Lim. Sparse directional image representations using the discrete shearlet transform, *Appl. Comput. Harmon. Anal.*, 25: 25–46, 2008.

[4] T. A. Gillette, K. M. Brown, and A. Ascoli. The DIADEM metric: comparing multiple reconstructions of the same neuron. *Neuroinformatics*, 9:233–245, (2011).

[5] D. Jiménez, E. Papadakis, D. Labate, and I. A. Kakadiaris. Improved automatic centerline tracing for dendritic structures. preprint, 2012

[6] F. Laezza, B.R. Gerber, J. Lou, M. Kozel, H. Hartman H, A. M. Craig, D. M. Ornitz, J. Nerbonne. The FGF14(F145S) mutation disrupts the interaction of FGF14 with voltage-gated Na^+ channels and impairs neuronal excitability. *J Neurosci.*, 27(44):12033–44, 2007.

[7] M. P. Mattson. Glutamate and neurotrophic factors in neuronal plasticity and disease. *Ann. N Y Acad. Sci.*, 1144:97-112, 2008.

[8] P. S. Negi and D. Labate, 3D discrete shearlet transform and video processing, *IEEE Trans. Image Process.* 21(6):2944–2954, 2012.

[9] Y. Wang, A. Narayanaswamy, C.-L. Tsai, and B. Roysam. A broadly applicable 3-D neuron tracing method based on open-curve snake. Neuroinformatics, 9(2-3):193-217, 2011.